




Stress biomarker detection with a grating-coupled surface plasmon resonance sensor

Anni Ranta-Lassila ^{a,*} Duc Le ^a Teemu Sipola,^a Mikko Karppinen,^a Jarno Petäjä,^a Minna Kehusmaa,^a Sanna Aikio,^a Tian-Long Guo,^b Matthieu Roussey,^b Jussi Hiltunen,^a and Alexey Popov ^a

^aVTT Technical Research Centre of Finland Ltd, Oulu, Finland

^bUniversity of Eastern Finland, Center for Photonics Sciences, Joensuu, Finland

ABSTRACT. Stress is a natural response of the body to threatening and challenging situations. Although stress can sometimes have positive impacts, such as enhanced alertness and improved performance, it can also cause harmful effects, such as sustained high blood pressure, anxiety, and depression, especially when prolonged. Continuous monitoring of stress-related molecules, known as stress biomarkers, could enable early diagnosis of stress conditions and therefore improve recovery and reduce healthcare costs and long absences from work. We present a highly sensitive grating-coupled surface plasmon resonance (SPR) sensor for detecting stress biomarkers. The gold-coated sensor chip operates with a tunable laser within the wavelength range of 1527 to 1565 nm. This sensing method is based on detecting a shift of the SPR wavelength, which occurs due to a change in the refractive index of the medium that is caused by the presence of analytes near the plasmonic grating. The sensor chip was tested with four stress-related biomarkers: glucose, creatinine, lactate, and cortisol. With the current version of the sensor, containing no recognition element, the achieved detection limits for these analytes were 5.9, 7.1, 36.9, and 10.7 mM, respectively, which are close to the physiological values of these analytes in body fluids, such as sweat. This proof-of-concept work demonstrates the sensitivity and physiologically relevant detection limits of the presented compact sensor chip and its potential for future healthcare applications, such as continuous stress monitoring, when developed further.

© The Authors. Published by SPIE under a Creative Commons Attribution 4.0 International License. Distribution or reproduction of this work in whole or in part requires full attribution of the original publication, including its DOI. [DOI: [10.1117/1.OE.63.11.117103](https://doi.org/10.1117/1.OE.63.11.117103)]

Keywords: stress biomarker; plasmonic sensing; surface plasmon resonance; grating-coupled surface plasmon resonance sensor

Paper 20240855G received Aug. 26, 2024; revised Oct. 14, 2024; accepted Oct. 23, 2024; published Nov. 15, 2024.

1 Introduction

Stress is a widely spread phenomenon in the modern society. Only work-related stress was estimated to cost U.S. companies more than \$300 billion a year in healthcare costs, absences, and decreased performance.¹ Work-related stress can cause both acute burnout and chronic stress. In addition to psychological stress, stress conditions can also be based on physical stress, such as in overtraining syndrome (OTS). OTS is a common condition among athletes whose prevalence varies between 5% and 60% during their career, depending on the sport and its intensity.² OTS is caused by excessive training and deficient recovery, and it leads to exhaustion and depleting performance.²

*Address all correspondence to Anni Ranta-Lassila, anni.ranta-lassila@vtt.fi

Table 1 Stress biomarker concentrations (mM) in different body fluids.

| Biomarker | Blood | Sweat | Saliva | Urine | Tears |
|------------|--|---|--|---|--|
| Glucose | 4.9 to 6.9 (Ref. 5) | 0.06 to 0.11 (Ref. 5) | 0.23 to 0.38 (Ref. 5) | 2.78 to 5.55 (Ref. 5) | 0.05 to 0.5 (Ref. 5) |
| Creatinine | 0.05 to 0.1 (Ref. 6) | 0.01 to 0.05 (Ref. 7) | 0.01 to 0.4 (Ref. 8) | 14.1 to 28.9 (Ref. 6) | 0.04 (Ref. 9) |
| Lactate | 0.5 to 2 (Ref. 10) | 16 to 30 (Ref. 11) | 0.2 to 0.5 (Ref. 12) | 0.5 to 2.5 (Ref. 13) | 1 to 5 (Ref. 14) |
| Cortisol | 0.1 to 0.8×10^{-3} (Ref. 15) | 0.02 to 0.4×10^{-3} (Ref. 15) | 2.8 to 4.4×10^{-6} (Ref. 15) | 0.03 to 0.3×10^{-3} (Ref. 15) | 0.01 to 0.11×10^{-3} (Ref. 16) |

Early diagnosis of stress conditions is crucial as the conditions are often not fully reversible. Early detection, improved recovery, and reduced healthcare costs could be achieved with continuous monitoring of stress biomarkers using wearable devices. Current commercially available wearable devices can measure various physical properties, such as pulse, body temperature, and blood oxygenation.³ However, the detection of molecular stress biomarkers is still mostly on the laboratory scale.⁴ These molecules are present in different body fluids, such as blood, sweat, saliva, urine, and tears, from where they can be detected with biosensors.⁴ When considering continuous, non-invasive monitoring, sweat is the most favorable fluid to detect biomarkers from. Table 1 presents concentrations of four stress-related biomarkers, glucose, creatinine, lactate, and cortisol, in different body fluids.

Both electrochemical and optical sensors, including plasmonic sensors, have been proposed for detecting glucose, creatinine, lactate, and cortisol in previous literature.^{17–19} Although electrochemical biosensors are closer to implementation in wearable devices due to their ease of fabrication, optical biosensors have recently attracted increasing attention in research.³ Optical sensors offer high sensitivity, high stability, and fast data collection but can be difficult to implement into compact wearable devices due to bulky or energy-consuming components.³ A solution to this issue could be in plasmonic optical sensing. Plasmonic sensing is based on plasmons that are oscillations of electron density in plasma.²⁰ Plasmons occur when electromagnetic radiation is directed to a plasmonic material, usually a metal, and electrons oscillate with respect to their positive ions.²⁰ Plasmons are sensitive to physical changes of the surrounding medium, such as its refractive index (RI), and can therefore be exploited in sensors.²⁰ Plasmonic sensors enable high sensitivity, integration into compact and energy-efficient devices, reusability, label-free detection, and short response time.³ Integration of a plasmonic sensor into a wearable device could enable continuous and non-invasive stress monitoring and, therefore, early detection of stress conditions.

Regarding plasmonic sensors, a common method for observing changes in the RI of a medium is surface plasmon resonance (SPR).²¹ In SPR sensors, a light beam of a certain wavelength, angle, and polarization is directed to a metal surface to induce plasmons, more specifically surface plasmon-polaritons (SPPs), which can propagate along a metal surface. Typically, the momentum of SPPs is higher than that of light in a sample.²⁰ Because of this momentum mismatch, SPPs cannot form on a smooth metal surface under normal incident light. To overcome this, various coupling techniques are used to increase the momentum of the light in the medium to match that of the SPPs. These techniques include high-index prism, grating, optical fiber, and waveguide coupling.²¹ Prism-based SPR sensors are widely used for research and industrial purposes. However, their large form factor limits their use in wearable health monitoring. Smaller-sized grating-based SPR sensors coupled with a compact tunable laser present a highly desirable solution, showing promise for miniaturized sensors suitable for wearable applications. Nonetheless, the lower physiological concentration of body analytes necessitates high sensitivity of SPR sensors for this to happen.

Although plasmonic biosensors have previously been developed to target various analytes, including metabolites,^{22–24} proteins,^{25–27} and viral DNA,^{28–30} detection of stress biomarkers, especially with grating-based SPR sensors and tunable lasers, has been relatively underexplored.

Here, we present a grating-coupled SPR sensor for the detection of four stress-related biomarkers: glucose, creatinine, lactate, and cortisol.^{31,32} The method is based on detecting an SPR wavelength shift due to an RI change of the medium caused by molecules of analytes in the vicinity of the plasmonic grating. Detection limits and sensitivities of the fabricated SPR sensor chips were revealed for the measured biomarkers. Deployment of the tunable laser makes the use of a spectrometer as a detector obsolete, further contributing to the compactness of the whole sensor. This work represents a proof of concept that demonstrates the sensitivity and physiologically relevant limits of detection of the sensor for multiple stress-related biomarkers. With further development, including laser miniaturization and the addition of a recognition element, the sensor could become a part of integrated sensor wearable devices.

2 Methods

2.1 Fabrication of SPR Sensor Chips

SPR sensor chips were designed using the COMSOL Multiphysics software (COMSOL, Stockholm, Sweden), considering fabrication limitations and tolerances that constrained the final design. We chose rectangular grating due to its ease of fabrication using scalable techniques, e.g., nanoimprinting. The design model is illustrated in Fig. 1(a). During the design process, we optimized three grating parameters, i.e., period, ridge width, and groove depth, to minimize the full width at half maximum (FWHM) of the SPR dip within the laser's tuning range. Therefore, the figure of merit, defined by the ratio between the sensitivity and the FWHM of the SPR dip, was maximized. Details of the design are provided in our previous paper.³³ As an example, simulation results of the SPR dip wavelength shift as a function of glucose concentration (in an aqueous solution) and RI change are presented in Fig. 1(b).

Briefly, the SPR sensor chips were fabricated as follows. The master template was fabricated on a 10-cm silicon wafer by e-beam lithography and etching. It includes 5 mm × 5 mm nano-grating areas with a ridge height of 55 nm and varying ridge widths and periods. A 10-cm glass working stamp was manufactured from the master by ultraviolet nanoimprinting lithography (UV-NIL) and a hybrid polymer material. With the help of the working stamp, the sensor replicas were manufactured on a 10-cm silicon wafer by UV-NIL and the hybrid polymer material. Subsequently, the sensor areas were coated with a 150-nm-thick gold layer by thermal evaporation and cut out from the wafer into ~1.5 cm × 1.5 cm pieces. The sensor chips and an illustration of their structure are presented in Figs. 2(a) and 2(b). The chips with a grating groove

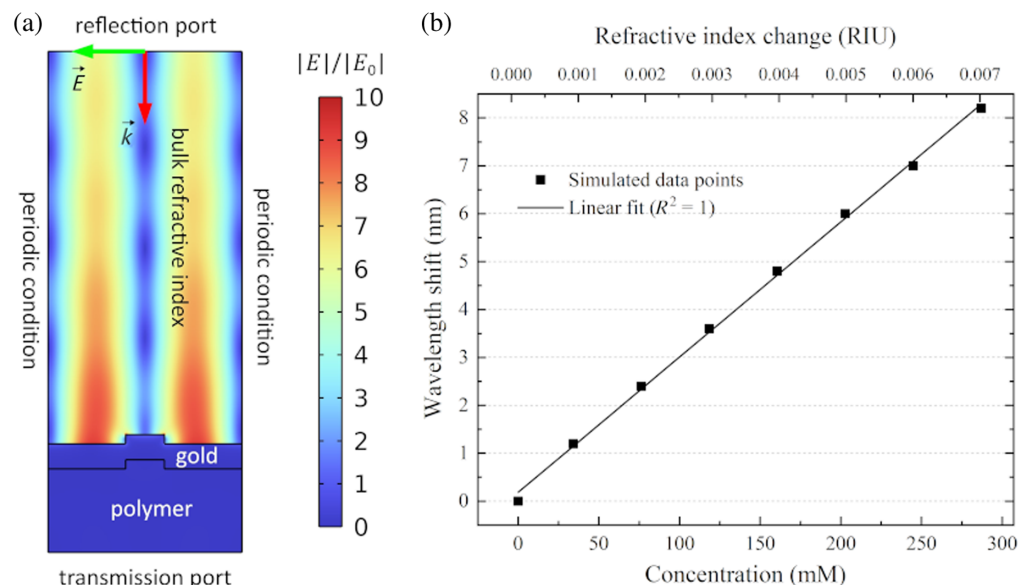


Fig. 1 (a) 2D model of the unit cell of the SPR chip used for the design process in COMSOL Multiphysics. (b) Simulation results of the SPR wavelength shift as a function of glucose concentration and the RI change.

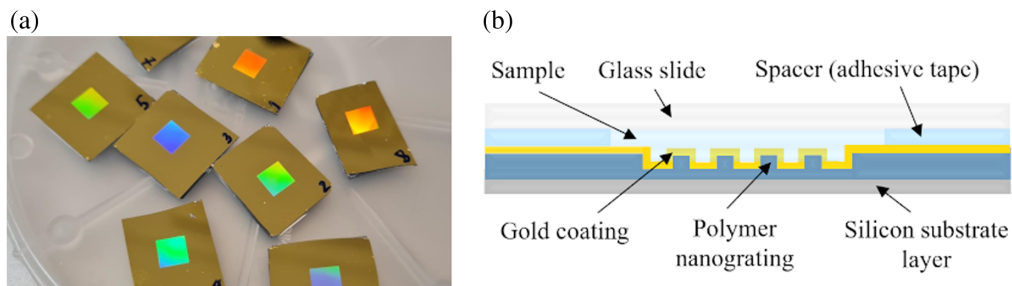


Fig. 2 (a) Gold-coated SPR sensor chips. (b) Illustration of the sensor structure (not to scale).

width of 232 nm and a period of 1160 nm showed a resonance dip in the desired wavelength range (1527 to 1565 nm). A more detailed fabrication process is described in our previous paper.³³

2.2 Measurement System

The measurement system and the principle of sensing are illustrated in Fig. 3, and the actual setup is shown in Figs. 4(a) and 4(b). Collimated, linearly polarized light from a tunable infrared (IR) laser was first directed onto the sample and then to a detector, through optical components, all purchased from Thorlabs. To record measurement data, an in-house developed LabVIEW-based software was used. The tunable laser TLX1 Tunable Laser Source (Thorlabs, Bergkirchen, Germany) emitted short-wavelength IR light in the range of 1527.6 to 1565.6 nm. A biased InGaAs photodetector (Thorlabs, Germany) registered light reflected from the sensor with samples.

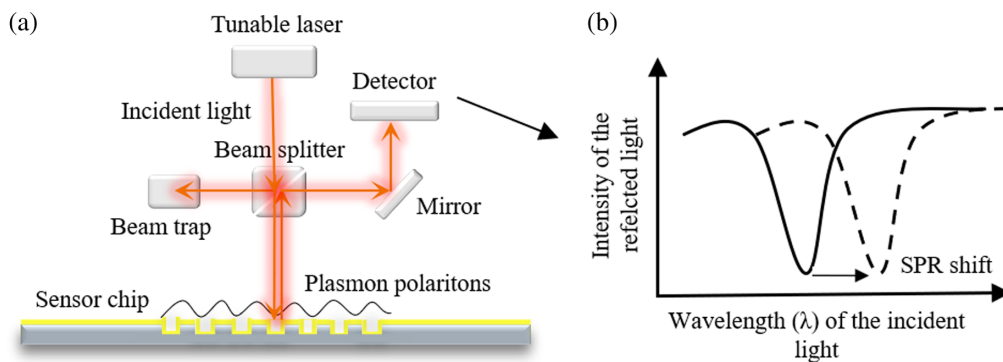


Fig. 3 (a) Schematic of the measurement system and (b) the sensing principle.

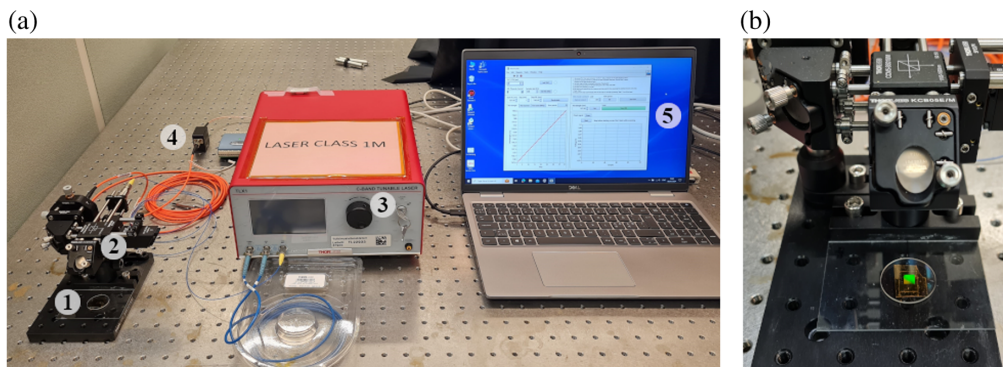


Fig. 4 (a) SPR setup. 1: sensor chip, 2: optical setup, 3: tunable laser, 4: detector, and 5: software. (b) Sensor chip in the optical setup, with the sensing area appearing green.

2.3 Sample Preparation and Measurements

Measurements were performed with the four stress biomarkers of interest: glucose, creatinine, lactate, and cortisol, all purchased from Sigma-Aldrich. Glucose, creatinine, and lactate were diluted in deionized water, whereas cortisol was diluted in 20% aqueous ethanol solution to achieve higher solubility. The sample concentrations ranged between 0 and 300 mM.

The sensor chips were taped onto sample holders to ensure the correct alignment of the gratings in the system. For each measurement, 30 μ l of the sample was pipetted on top of the SPR chip. A 1-mm-thick glass cover was set on top of the sample to achieve an even sample surface. The cover had an anti-reflection coating on both sides to prevent interference between the incident and the reflected light. An adhesive tape also worked as a spacer between the sensor and the glass cover.

3 Results

Experiments were conducted using the four biomarkers and two different sensor chips (1 and 2) to characterize their sensing performance as well as the effect of fabrication tolerances. Figure 5(a) presents the SPR signal in the presence of deionized water (concentration 0 mM) with these two sensor chips, and Fig. 5(b) shows the SPR signal from chip 2 in the presence of 30-mg/ml glucose, creatinine, and lactate.

The SPR wavelength corresponds to the position of the intensity minimum of each curve. This position depends on the target analyte and its concentration. The SPR wavelength shift is the difference among the positions of the SPR wavelength at different analyte concentrations. Different locations of the SPR wavelength among different sensor chips do not affect the accuracy of measurements because the SPR technique relies on detecting relative changes in the SPR wavelength rather than its absolute position.

To analyze the SPR shift for the analytes and the sensitivities of the sensor chips, linear regressions of the resonance points were compiled. The linear fittings for glucose, creatinine, and lactate with chips 1 and 2 are presented in Fig. 6. For the regression analysis, the average resonance points of the three samples for each concentration were calculated. The SPR wavelengths were determined using the minimum of the reflectance data, and the corresponding wavelength shifts were calculated relative to the SPR wavelength at the baseline (0 mM concentration in deionized water). For glucose, the simulation data are also shown.

Figure 6 shows that the SPR wavelength shifts increase linearly with the sample concentrations. The R^2 values, ranging from 0.93 to 1, indicate an excellent fit of the data to the regression lines. The simulated data for glucose also aligns well with the experimental results. To assess the performance of the sensor, limits of detection (LODs) and sensitivities were calculated for the analytes and the sensor chips. The tested sensor chips, analytes, measured concentrations, sensitivities, and LODs are presented in Table 2 (higher concentrations).

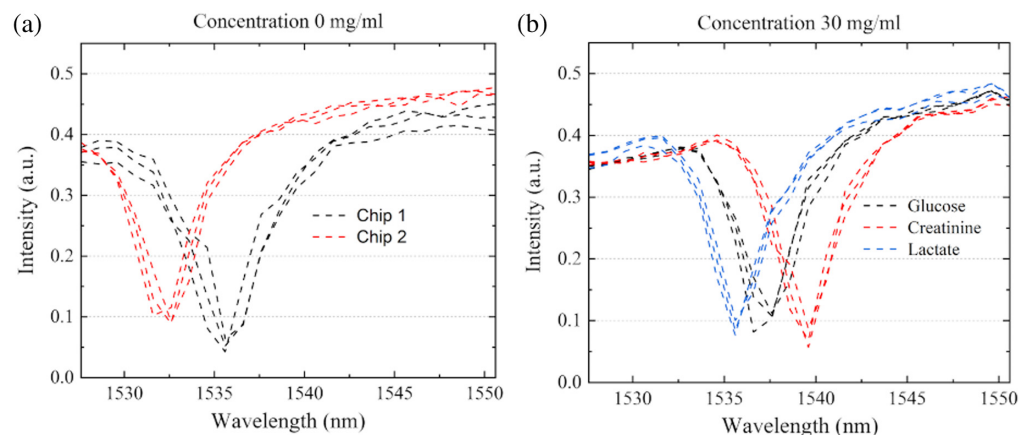


Fig. 5 (a) SPR signal in the presence of deionized water with the two tested sensor chips. (b) SPR signal in the presence of glucose, creatinine, and lactate with sensor chip 2 and concentrations of 30 mg/ml.

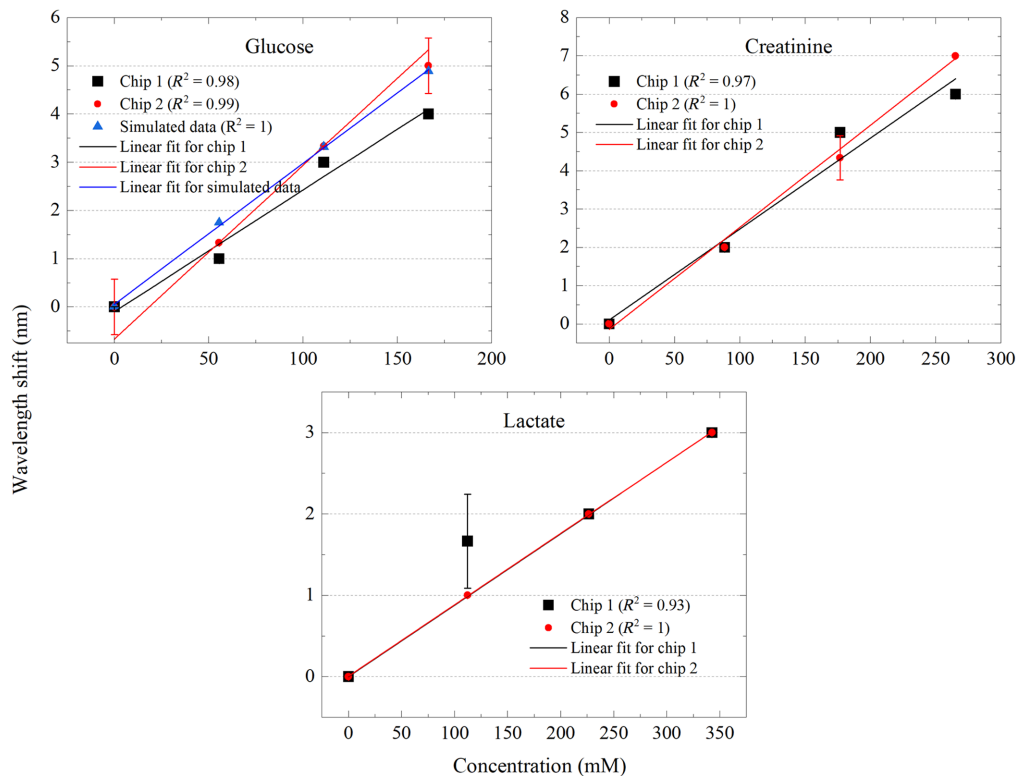


Fig. 6 Linear fittings of the SPR wavelength shift in the presence of glucose, creatinine, and lactate (chips 1 and 2). For glucose, a comparison between experimental and simulated data is shown.

Table 2 Sensitivities and LODs of the SPR sensor for glucose, creatinine, and lactate (higher concentrations). Higher sensitivity and lower LOD results for each analyte are in bold.

| Sensor chip | Analyte | Measured concentrations (mM) | Sensitivity ($\frac{\text{nm}}{\text{mM}}$) | LOD (mM) |
|-------------|------------|------------------------------|---|---|
| 1 | Glucose | 0, 56, 111, and 167 | 0.030 | 13.32 |
| 2 | | | 0.031 | 17.78 |
| 1 | Creatinine | 0, 88, 177, and 265 | 0.024 | 68.76 |
| 2 | | | 0.026 | 24.66 |
| 1 | Lactate | 0, 111, 223, and 334 | 0.008 | 129.97 |
| 2 | | | 0.009 | 8.73×10^{-8} |

In Table 2, the achieved LODs are below the lowest tested concentrations of the analytes (except 0 mM concentration), indicating potential improvement with more precise testing. Therefore, the concentrations and the wavelength step size were decreased. Concentrations of 0 to 56 mM, 0 to 88 mM, 0 to 111 mM, and 0 to 8 mM were tested with glucose, creatinine, lactate, and cortisol, respectively. After revealing approximate SPR wavelengths with prior tests, the wavelength step size was decreased from 1 to 0.1 nm to achieve more accurate results. Linear fittings of the SPR wavelength shifts with lower analyte concentrations and smaller concentration gradients are shown in Fig. 7.

With lower concentrations and a smaller wavelength step size, the average SPR wavelength shifts do not align with their linear fittings as well as with the higher concentration samples. Although glucose and creatinine are still relatively well-fitted, the R^2 values of lactate and cortisol are notably lower (0.79, 0.79; 0.42, 0.61). However, for cortisol, the concentrations are

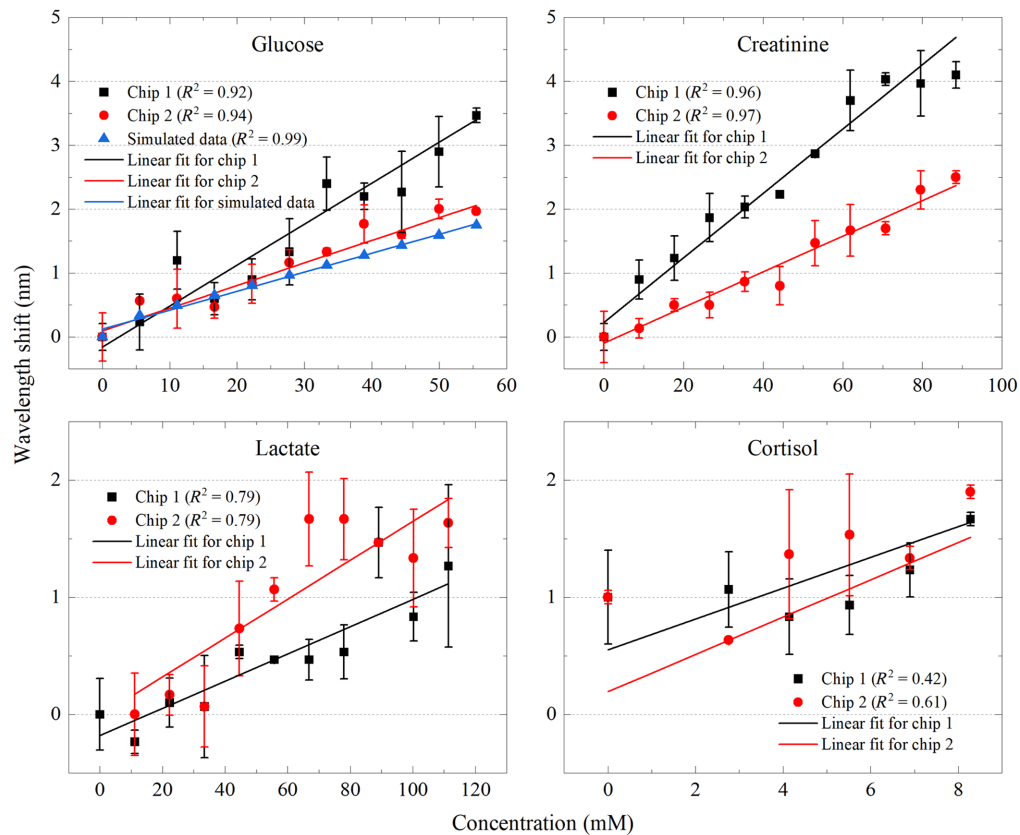


Fig. 7 Linear fittings of the SPR wavelength shift in the presence of lower concentrations of glucose, creatinine, lactate, and cortisol (chips 1 and 2). For glucose, a comparison between experimental and simulated data is shown.

much lower than for the other analytes due to the low solubility of cortisol in water. The simulated data for glucose also aligns well with experimental results (chip 2).

The tested sensor chips, the measured concentrations, and the calculated sensitivities and LODs for these lower concentrations are presented in Table 3. With the lower concentrations and the smaller wavelength step size, the sensitivity and LOD values improved and the variation among the chips decreased compared with the larger concentrations (Table 2). When comparing chips 1 and 2, for both smaller and larger concentrations and both sensitivities and LODs, better

Table 3 Sensitivities and LODs of the SPR sensor for glucose, creatinine, lactate, and cortisol (lower concentrations). Higher sensitivity and lower LOD results for each analyte are in bold.

| Sensor chip | Analyte | Measured concentrations (mM) | Sensitivity ($\frac{\text{nm}}{\text{mM}}$) | LOD (mM) |
|-------------|------------|---|---|--------------|
| 1 | Glucose | 0, 6, 11, 17, 22, 28, 33, 39, 44, 50, and 56 | 0.036 | 8.91 |
| 2 | | | 0.077 | 5.89 |
| 1 | Creatinine | 0, 9, 18, 27, 35, 44, 53, 62, 71, 80, and 88 | 0.047 | 11.47 |
| 2 | | | 0.029 | 10.65 |
| 1 | Lactate | 0, 11, 22, 33, 45, 56, 67, 78, 89, 100, and 111 | 0.013 | 36.89 |
| 2 | | | 0.018 | 41.83 |
| 1 | Cortisol | 0, 3, 4, 6, 7, and 8 | 0.065 | 10.37 |
| 2 | | | 0.114 | 7.09 |

results were more often achieved with chip 2, specifically 6 out of 7 times for the sensitivity values and 5 out of 7 times for the LOD values.

4 Discussion

During the experiments, various fabricated sensor chips and analytes were tested. The simulated wavelength shift values for glucose corresponded well with the experimental data, showing well-performed fabrication and experiments. With higher analyte concentrations (~50 to 300 mM), larger concentration differences within the same analyte (~85 mM), and a larger measurement step size (1 nm), the SPR wavelengths increased almost linearly with the analyte concentrations. Expectedly, with lower concentrations (~5 to 100 mM), smaller concentration differences within the same analyte (~7 mM), and a smaller measurement step size (0.1 nm), the SPR wavelength increase had a higher deviation from the linear form. This is due to the increased impact of errors, which becomes more pronounced when working with finer concentration gradients and smaller measurement increments. When comparing the analytes, the linear model fits glucose and creatinine better than lactate and cortisol. The R^2 values for the fittings range notably between 0.42 and 0.97.

Both the sensitivities of the SPR chips and their LOD values vary over the chips and the analytes. Besides the structural differences of the chips, there are some other factors presumably affecting the results. These uncertainties include possible errors in both sample preparation and measurements. During sample preparation, errors can occur from analyte impurities, laboratory device calibration errors, and human errors. During measurements, uncertainties arise from slight laser instability, alignment of the sensor chip in the setup, and sample heating under laser irradiation. In the future, the measurement uncertainties could be diminished using a more stable tunable laser, ensuring correct alignment of the sensor chip in the setup with mechanical alignment and preventing sample heating with thermal stabilization.

When comparing the achieved LOD values with the actual concentrations of stress biomarkers in body fluids (Table 1), it is evident that some LOD values align with the actual concentrations of these analytes in certain body fluids. Specifically, the glucose LOD falls within the concentration range found in the blood and is very close to that in urine. The LOD for creatinine is below the concentration range in urine, whereas for lactate, it is near the concentration range found in sweat. These results highlight the future capabilities of the presented sensor for continuous body fluid monitoring. Consequently, further development of the sensor will involve testing with body fluids, starting with artificial samples and later using human-derived fluids.

The LODs of the previously presented SPR sensors in the literature are in the micromolar or even nanomolar range.²²⁻²⁴ Compared with the sensors in previous studies, a significant distinction of the sensor proposed in this work is the absence of a receptor layer. Considering that the sensing is solely based on the plasmonic effect of electron oscillations and not on biological target-receptor binding, the LODs at the mM level are reasonable. In the future, incorporating an additional sensing element in the sensor structure would notably improve the sensitivity and also enable selectivity.

5 Conclusions

Here, we demonstrated a grating-coupled SPR sensor for stress biomarker detection. The sensor comprised a polymeric nanograting on a silicon substrate covered with gold. The sensor was tested with four stress-related biomarkers: glucose, creatinine, lactate, and cortisol. The presented sensor showed a visible plasmonic shift with all the tested analytes. For higher (~50 to 300 mM) and lower concentrations (~5 to 100 mM), a close to linear increase of the SPR wavelength shift versus concentration was achieved with glucose and creatinine.

Detection limits of 5.89, 10.65, 36.89, and 7.09 mM were achieved for glucose, creatinine, lactate, and cortisol, respectively. Compared with other sensors previously reported in the literature for detecting these stress biomarkers, our sensor did not reach similar detection limits, which can be associated with the absence of the receptor layer. Adding a sensing element to the sensor structure would increase sensitivity and enable the selectivity of the SPR sensor. However, the detection limits of our sensor for glucose, creatinine, and lactate reached their

physiological concentrations in blood, urine, and sweat, respectively. This shows the promise of our SPR sensor for continuous body fluid monitoring. With further development, our SPR sensor has the potential for personalized health monitoring and could be used as a tool for diagnosing stress conditions, such as burnout and OTS.

Disclosures

The authors declare that there are no financial interests, commercial affiliations, or other potential conflicts of interest that could have influenced the objectivity of this research or the writing of this paper.

Code and Data Availability

Data are available from the authors after a reasonable request and after permission from the authors' organizations.

Acknowledgments

This work was funded by VTT Technical Research Centre of Finland (WearHealth Project No. 135634), Business Finland (PHOTON WEAR Project No. 136954) and the Research Council of Finland (PREIN Flagship, Decision No. 346545). ChatGPT by OpenAI was used for slight grammar improvements.

References

1. "Financial costs of job stress," UMass Lowell, <https://www.uml.edu/research/cph-new/worker/stress-at-work/financial-costs.aspx> (accessed 04 March 2024).
2. J. B. Kreher, "Diagnosis and prevention of overtraining syndrome: an opinion on education strategies," *Open Access J. Sports Med.* **7**, 115–122 (2016).
3. B. Kaur, S. Kumar, and B. K. Kaushik, "Novel wearable optical sensors for vital health monitoring systems—a review," *Biosensors* **13**(2), 181 (2023).
4. B. Senf, W. Yeo, and J. Kim, "Recent advances in portable biosensors for biomarker detection in body fluids," *Biosensors* **10**(9), 127 (2020).
5. D. Bruen et al., "Glucose sensing for diabetes monitoring: recent developments," *Sensors* **17**(8), 1866 (2017).
6. "Creatinine blood test," Mount Sinai Health System, <https://www.mountsinai.org/health-library/tests/creatinine-blood-test> (accessed 04 October 2024).
7. C. Huang et al., "Uric acid and urea in human sweat," *Chin. J. Physiol.* **45**(3), 109–115 (2002).
8. D. O. Temilola et al., "Salivary creatinine as a diagnostic tool for evaluating patients with chronic kidney disease," *BMC Nephrol.* **20**, 387 (2019).
9. S. Zhou et al., "An eco-friendly hydrophilic interaction HPLC method for the determination of renal function biomarkers, creatinine and uric acid, in human fluids," *Anal. Methods* **5**, 1307–1311 (2013).
10. "UC Davis Health: lactate profile," <https://health.ucdavis.edu/sports-medicine/resources/lactate> (accessed 04 October 2024).
11. P. J. Derbyshire et al., "Lactate in human sweat: a critical review of research to the present day," *J. Physiol. Sci.* **62**, 429–440 (2012).
12. D. K. Shruthi et al., "The role of salivary lactate levels in assessing the severity of septic shock," *J. Oral Maxillofac. Pathol.* **25**(3), 437–440 (2021).
13. I. Kosmidis et al., "Reliability of the urine lactate concentration after alternating-intensity interval exercise," *Proceedings* **25**(1), 1 (2019).
14. C. Lin et al., "Development toward a novel integrated tear lactate sensor using Schirmer test strip and engineered lactate oxidase," *Sens. Actuators B: Chem.* **270**(1), 525–529 (2018).
15. A. J. Steckl and P. Ray, "Stress biomarkers in biological fluids and their point-of-use detection," *ACS Sens.* **3**(10), 2025–2044 (2018).
16. M. Ku et al., "Smart, soft contact lens for wireless immunosensing of cortisol," *Sci. Adv.* **6**(28), eabb2891 (2020).
17. R. M. Torrente-Rodriguez et al., "Investigation of cortisol dynamics in human sweat using a graphene-based wireless mHealth," *Matter* **2**(4), 921–937 (2020).
18. J. Choi et al., "Soft, skin-integrated multifunctional microfluidic systems for accurate colorimetric analysis of sweat biomarkers and temperature," *ACS Sens.* **4**(2), 379–388 (2019).
19. H. S. Kim et al., "Hand-held Raman spectrometer-based dual detection of creatinine and cortisol in human sweat using silver nanoflakes," *Anal. Chem.* **93**(45), 14996–15004 (2021).

20. E. Le Ru and P. Etchegoin, *Principles of Surface-Enhanced Raman Spectroscopy*, pp. 121–183, Elsevier Science, Oxford, UK (2009).
21. A. M. Shrivastav, U. Cvelbar, and I. Abdulhalim, “A comprehensive review on plasmonic-based biosensors used in viral diagnostics,” *Commun. Biol.* **4**(1), 70 (2021).
22. H. Yuan et al., “Fiber-optic surface plasmon resonance glucose sensor enhanced with phenylboronic acid modified Au nanoparticles,” *Biosens. Bioelectron.* **117**, 637–643 (2018).
23. M. Soares et al., “Label-free plasmonic immunosensor for cortisol detection in a D-shaped optical fiber,” *Biomed. Opt. Express* **13**(6), 3259–3274 (2022).
24. P. Sharma, V. Semwal, and B. Gupta, “Fiber optic surface plasmon resonance based lactate sensor using co-immobilization of lactate dehydrogenase and NAD+,” *Opt. Fiber Technol.* **49**, 22–27 (2019).
25. B. Hinkov et al., “A mid-infrared lab-on-a-chip for dynamic reaction monitoring,” *Nat. Commun.* **13**, 4753 (2022).
26. Q. Wang, J. Jing, and B. Wang, “Highly sensitive SPR biosensor based on graphene oxide and staphylococcal protein A co-modified TFBG for human IgG detection,” *IEEE Trans. Instrum. Meas.* **68**(9), 3350–3357 (2019).
27. M. Soler et al., “Label-free SPR detection of gluten peptides in urine for non-invasive celiac disease follow-up,” *Biosens. Bioelectron.* **79**, 158–164 (2016).
28. H. Bai et al., “A SPR Aptasensor for detection of avian influenza virus H5N1,” *Sensors* **12**(9), 12506–12518 (2012).
29. W. Gong et al., “Experimental and theoretical investigation for surface plasmon resonance biosensor based on graphene/Au film/D-POF,” *Opt. Express* **27**, 3483–3495 (2019).
30. D. Silvestri et al., “A peptide nucleic acid label-free biosensor for Mycobacterium tuberculosis DNA detection via azimuthally controlled grating-coupled SPR,” *Anal. Methods* **7**(10), 4173–4180 (2015).
31. A. Ranta-Lassila et al., “SPR-based sensing of physiological analytes using a tunable laser: towards wearable applications,” *Proc. SPIE* **12860**, 1286003 (2024).
32. A. Ranta-Lassila et al., “Detection of stress biomarkers cortisol and creatinine with a grating-coupled surface plasmon resonance sensor,” *Proc. SPIE* **12991**, 1299111 (2024).
33. D. Le et al., “High-performance portable grating-based surface plasmon resonance sensor using a tunable laser at normal incidence,” *Photonics Res.* **12**, 947–958 (2024).

Anni Ranta-Lassila is a starting research scientist at VTT Technical Research Centre of Finland. Her main focus is on biosensing-related plasmonics and phantoms. She received her MSc degree in biomedical engineering from Aalto University in 2024.

Duc Le has a master’s degree in photonics. Currently, Duc Le is a research scientist at VTT Technical Research Centre of Finland and a doctoral candidate at the University of Eastern Finland. His research is to apply plasmonics in biosensing.

Jarno Petäjä received his MSc degree in physics from the University of Oulu, Finland, in 2003. He has been a research scientist at VTT Technical Research Centre of Finland for more than 20 years. Most of the focus has been related to micro- and nanoscale manufacturing, process development, and surface topography in the fields of printed electronics and optics, co-fired ceramics, photonics packaging, microfluidics, biosensors, photolithography, and nanoimprinting.

Jussi Hiltunen acts as a research professor at VTT Technical Research Centre of Finland. He has over 20 years of experience in photonic microsystems, with a particular interest in the development of integration technologies for healthcare applications, such as wearable devices and *in vitro* diagnostics solutions.

Alexey Popov is a research professor at VTT Technical Research Centre of Finland. He was trained as a physicist, with an emphasis on biomedical optics (biophotonics), laser physics, and spectroscopy. His scientific activity focuses on the development of wearable and portable optical sensing solutions for biomedical diagnostics and wellness. He is the author of 150 papers in international peer-reviewed scientific journals and conference proceedings, 5 book chapters, and over 200 presentations at major international conferences.

Biographies of the other authors are not available.